*Highlights (for review)

RESEARCH HIGHLIGHTS

- I present a new model of post-Jurassic plate motion in SW Gondwana.
- The model does not require small plates to open or close the Rocas Verdes Basin.
- The Patagonian orocline containing the basin remnants is a crustal-scale product of oblique plate convergence.

*Graphical Abstract (for review)

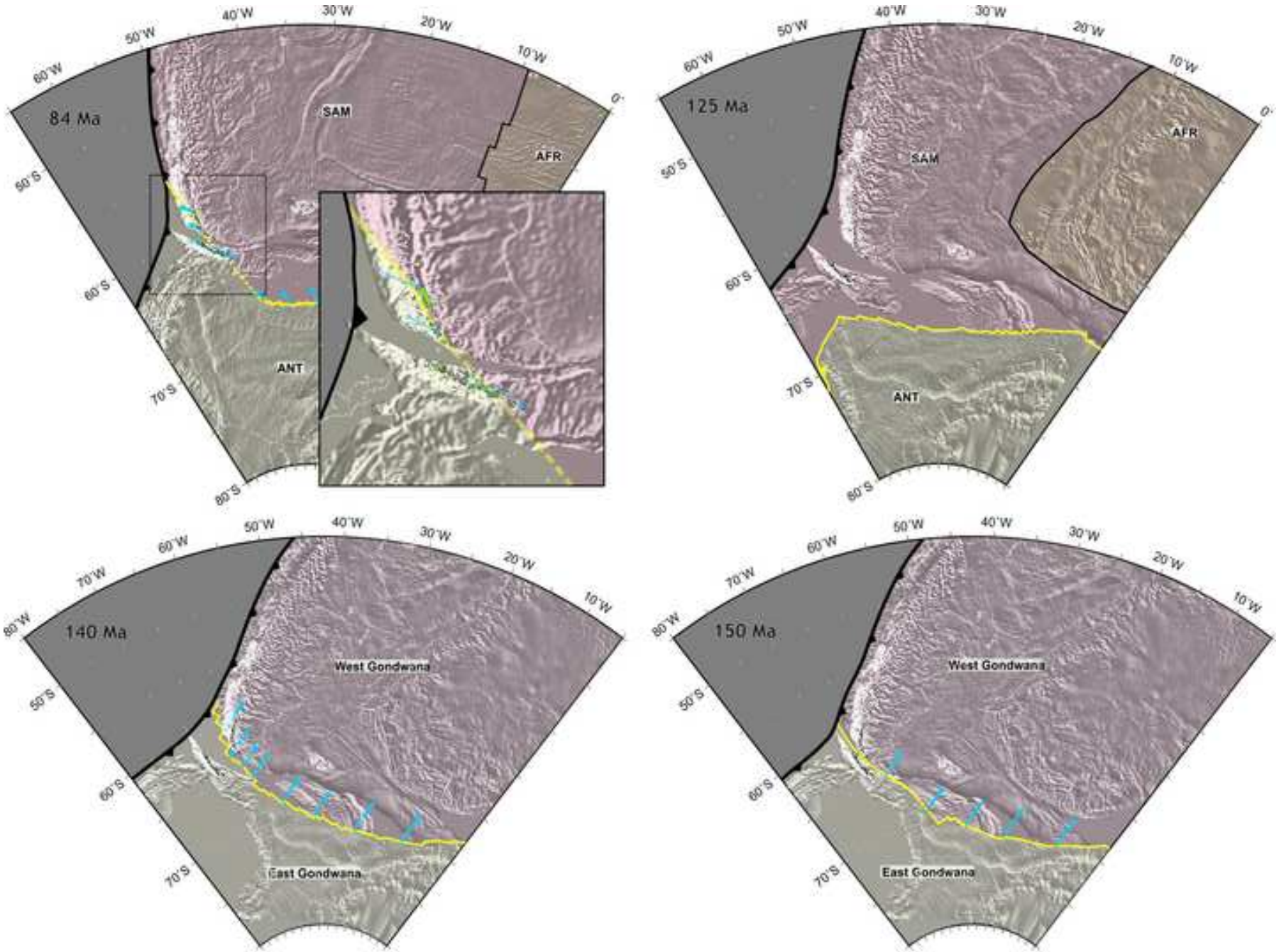

*Revised manuscript with no changes marked
Click here to view linked References

Plate kinematics of the Rocas Verdes Basin and Patagonian orocline

Graeme Eagles

Keywords: ***Weddell Sea, seafloor spreading, plate tectonics, Rocas Verdes Basin, Patagonian orocline***

Alfred Wegener Institut, Helmholtz Zentrum für Polar and Meerschweinchen
Am Alten Hafen 26
27568 Bremerhaven
Germany
Email: geagles@awi.de

ABSTRACT

The processes of orocline formation are a topic of debate in geosciences. The Patagonian orocline has been a case in point for over a century. Large anomalous paleomagnetic pole rotations show that the orocline started to form at the same time as mid-Cretaceous closure of the Rocas Verdes Basin, today known from ophiolitic and basin fill remnants in the Patagonian and Fuegian Andes. Some studies therefore present bending of the Andes and closure of the basin as shared consequences of rotation of a small plate that was driven by subduction-related forces at the Pacific margin of Gondwana. An alternative view of the orocline is as a product of Cretaceous to Paleogene-aged sinistral oblique convergence at the plate-boundary scale. Geological data from Tierra del Fuego have been interpreted in support of both views. Here, I test these suggestions by comparing the Rocas Verdes Basin's tectonostratigraphy to predictions of a plate kinematic model for fragmentation of the western interior of Gondwana. The model is sufficient to explain the known history of basin opening to a width of ~100-300 km during the period 152-141 Ma and later closure in oblique plate convergence. As this convergence occurred by motion around a distant Euler pole, it could not have produced the Patagonian orocline by rotation of a lithospheric plate on its Pacific flank. The large anomalous paleomagnetic rotations of Tierra del Fuego, instead, are likely to have occurred within the crust by rotation and deformation of regional strike-slip faults and the intervening rocks to accommodate oblique convergence of the South American and Antarctic plates between Albian and Paleocene times.

1. INTRODUCTION

Oroclines result from tectonic bending of mountain ranges, requiring segments of them to rotate. Early definitions assumed mountain ranges to originally form as linear features, and oroclines to be the results of their subsequent bending (*Carey*, 1955). Later definitions, recognizing the complexity and longevity of orogenesis, have required only that bending by rotation about a vertical axis be demonstrated (*Marshak*, 1988). The Patagonian orocline is the ~90° bend in the southernmost Andes that was presented in the late 19th century as part of a much larger isoclinal fold whose limbs constitute the northern and southern ridges of the Scotia Arc (*Arctowski*, 1885). Although the existence of such a fold has since been disproved, paleomagnetic data have repeatedly confirmed rock rotations about vertical axes in Tierra del Fuego, most markedly to the south of the Magallanes-Fagnano and Beagle Channel fault systems (Figure 1a; *Cunningham* et al., 1991; *Poblete* et al., 2014; 2016; *Rapalini* et al., 2015). The oldest known of these paleomagnetic rotations affect rocks of early to mid-Cretaceous age (e.g. *Poblete* et al., 2016). These, and related rocks, also document the latest Jurassic to early Cretaceous growth of a basin floored by oceanic crust, the Rocas Verdes Basin, and its subsequent closure by tectonic compression (e.g. *Klepeis* et al., 2010). The timing coincidence suggests that the basin history and oroclinal bending share a tectonic context.

This context, however, is not interpretable uniquely or in detail from the deformed remnants of the Rocas Verdes Basin, but instead must be inferred based on its wider setting. On this basis the basin is traditionally considered to have opened as a back-arc basin and closed in response to changes in relative motions of South America and the trench at its paleo-Pacific margin as the South American plate accelerated westwards over the mantle (*Dalziel*, 1981; *Somoza and Zaffarana*, 2008). It has been suggested that the basin's closure involved motion of a small lithospheric plate about an Euler pole that lay close by to the north (Figure 1c). The basis of this suggestion is in structural studies of thrust sheets in the southernmost Andes, whose arrangement can be explained by collision of Patagonia with a rotating indentor that comprised the internal domain of the Fuegian fold and thrust belt (*Kraemer,* 2003; *Ghiglione and Cristallini*, 2007; *Poblete* et al., 2016; *Torres Carbonell* et al., 2014; 2016).

None of these studies considers strike-slip motion, and yet vertical axis rock rotations are understood to be an inescapable consequence of rock translation and deformation between

working strike-slip faults (e.g. *Freund*, 1974; *Ron* et al., 1984). Evidence for sinistral strike-slip is widespread in Tierra del Fuego, with some consensus that a few tens of kilometres of strike-slip displacement have accumulated on the Magallanes-Fagnano fault zone since Oligocene times as part of the Scotia-South America plate boundary (e.g. *Klepeis*, 1994; *Klepeis and Austin*, 1997; *Lodolo* et al., 2003; *Eagles* et al., 2005; *Torres Carbonell* et al., 2008). In contrast, there is less agreement on the timing or magnitude of pre-Neogene strike-slip deformation (e.g. *Betka* et al., 2016). One school of thought concentrates on the observation that the evidence for Oligocene strike-slip widely overprints that for Cretaceous thrusting, and so surmises that strike-slip in Tierra del Fuego succeeded an earlier period of orthogonal convergence. An alternative viewpoint, concentrating on observations in the Beagle Channel region, is that a component of strike-slip has been accommodated since Cretaceous times (*Cunningham* 1993; 1995; *Menichetti* et al., 2008; *Klepeis* et al., 2010). Here, cross-cutting relationships with late Cretaceous plutons have been used to suggest that strike-slip faulting post-dates 73 Ma (*Klepeis* et al., 2010), but also that mid-Cretaceous ductile deformation produced sub-horizontal stretching lineations in zones of mylonitic foliation. Based on this latter interpretation, *Cunningham* (1993; 1995) concluded that the Patagonian orocline started to form at a mid-Cretaceous plate boundary that accommodated sinistral oblique motion between South America and the Antarctic Peninsula (Figure 1b).

Theoretically, the distribution of the magnitudes of paleomagnetic rotations could be useful to distinguish between the two proposed contexts for orocline development. Upper crustal rock rotations between strike-slip faults might be expected to vary in time and space depending on fault slip and spacing (*Freund*, 1974), whereas those caused by lithospheric plate rotation must be regionally homogeneous for any time slice. In Tierra del Fuego, however, the distribution of available rotations and their uncertainties do not allow for a confident analysis of the rotations' magnitude distribution at times before late Cretaceous (*Rapalini* et al., 2015; *Poblete* et al, 2016; Figure 1).

In summary, available geological constraints on the closure of the Rocas Verdes Basin and Cretaceous deformation of Tierra del Fuego are interpretable in terms of either of two separate mechanisms that acted to bend the southernmost Andes and form the Patagonian orocline. Complementary tests of these mechanisms are therefore necessary. In the following, I use a plate kinematic model to carry out such tests for (i) the necessity of

independent motions of small plates at the Pacific margin of Gondwana for the formation and destruction of the Rocas Verdes Basin and (ii) the occurrence of Cretaceous strike-slip tectonics in Tierra del Fuego as proposed by *Cunningham* (1993).

2. INVERSE MODEL FOR WEDDELL SEA PLATE MOTIONS

As well as placing it at Gondwana's paleo-Pacific margin, global plate reconstructions (e.g. *Dalziel* et al., 2013) portray the Rocas Verdes Basin as a geographical continuation of the Weddell Sea, a region of oceanic crust that formed by plate divergence in the fragmentation of the supercontinent. A simple plate kinematic interpretation of the Rocas Verdes Basin is thus as a feature that formed to accommodate divergence of the same pair of plates as at the Weddell Sea's mid-ocean ridge. This interpretation can be consistent with the apparent contradiction between the basin's back-arc location and the absence of active arc magmatism during its growth (*Caldéron* et al., 2003). *Livermore* et al. (2005) summarize work that demonstrated the plates separating in the Weddell Sea had been the South America and Antarctica plates since 84 Ma. A similar approach has been applied qualitatively to data from the older parts of the Weddell Sea, showing them also to be consistent with separation of the same two plates, or their parental plates West and East Gondwana, since the supercontinent's breakup (*König and Jokat*, 2006; *Eagles and Vaughan*, 2009). In the following, I use this premise to derive a data set that describes South American—Antarctic relative plate motions since Jurassic times. Afterwards, I consider the history of the Rocas Verdes Basin and its vertical axis rock rotations within the context of a plate kinematic model built using those data.

2.1. Isochron Data

Figure 2 shows the set of magnetic anomaly profiles from which picks of seafloor isochrons in the Weddell Sea were taken. In the northern parts of the Weddell Sea, isochrons can be confidently identified in a sequence beginning with chron 33 (*Livermore and Woollett*, 1993; *Livermore* et al., 2005). Within this framework, I picked a selection of the older ("o"; Table 1) or younger ("y") edges of well-defined anomalies. Where slow spreading rates lead to these edges being obscured by partial superposition of anomalies 28 to 21, I picked the anomaly peaks ("P") instead. No data younger than chron 8 (26.2 Ma) were picked facing the Endurance Collision Zone in view of inferences that the South America plate may have fragmented as segments of the ancestral South American–Antarctic Ridge approached the collision zone (*Menard*, 1978; *Barker et al*, 1984). Locations from north and west of the South

American-Antarctic Ridge, from which data are assigned to the South American plate, have been shown to be currently moving independently of it as part of the Sur component plate (*DeMets* at al., 2010). I found that their inclusion does not significantly affect the solution for South America-Antarctica motion, suggesting that the motion of Sur has not been large. In the southeast and south central Weddell Sea, picks of isochrons 340 to M15 (124.6–140.6 Ma) are based on the schemes of *Livermore and Hunter* (1996), *Jokat et al.*, (2003) and *König and Jokat*, (2006). In the southwest, close to the Antarctic Peninsula, anomalies in the magnetic data set are too diffuse to interpret confidently (*Barker and Jahn*, 1980; *LaBrecque and Barker,* 1981; *Ghidella* et al. 2002).

I additionally picked three undated targets (I, I2, MAU; Figure 3) (*Sandwell* et al., 2014). MAU is picked from the gravity anomaly at the northwestern margin of Maud Rise, part of a Cretaceous large igneous province that formed over the Bouvet plume and fragmented at the South American—Antarctic plate boundary. I and I2 are picked from gridded (*Golynsky* et al., 2001) magnetic intensity highs that occur over seafloor that formed during the Cretaceous normal polarity magnetic superchron. Although seafloor of this age is well known not to raise magnetic reversal anomaly isochrons, I and I2 may represent isochronous or near-isochronous processes that are unrelated to field reversals, such as geomagnetic field intensity variations (e.g. *Granot* et al., 2012) or magmatic pulses migrating along the ridge crest following variations in the material flux of the Bouvet mantle plume. The true process responsible for I and I2 is less important here than the fact that using these 48 data allows the model to be constrained by an additional 132 data from fracture zone azimuths developed in the Cretaceous normal polarity seafloor.

Finally, in order to extend the model back towards the Weddell Sea's continent-ocean transition zone, I picked targets at the northern edge of the Orion–Andenes magnetic anomaly, labelling them ORI, and at the gravity effect of the Weddell Sea shelf edge, labelling them WSE.

2.2. Fracture Zone data

Figure 2 shows free-air gravity anomalies in the region and the set of fracture zone interpretations made from them for use in the inversion. Numerous closely spaced fracture zones can be interpreted in these data north of a discontinuity known as Anomaly T (*Livermore and Hunter*, 1996; *Livermore* et al., 2005). South of Anomaly T, the anomaly field

is characterised by gentler oscillations with variable trends. *König and Jokat* (2006) chose not to consider any of these trends in their modelling of the tectonic development of the Weddell Sea, relying instead on their high-resolution magnetic anomaly isochrons. *Eagles and Vaughan* (2009) later showed that some of these anomalies are oriented as would be expected of fracture zones formed during the separation of east from west Gondwana. Despite the low amplitudes, therefore, the anomaly field south of Anomaly T presents valuable constraints on plate motion. I picked one of these anomalies as the expression of a fracture zone in the older parts of the Weddell Sea in order to allow the inversion to use the valuable fracture zone constraint whilst still being dominated by picks from the high-quality magnetic data of *Jokat* et al. (2003).

2.3. Inversion

I used the data set in an inversion that makes non-conjugate fitting of magnetic anomalies (cf. *Livermore et al*, 2005) simultaneously with iteratively improving the fit of a set of synthetic ridge-crest flowlines to the fracture zone locations. Non-conjugate fits were necessary in the absence of data from parts of the South American plate that were subducted beneath the Scotia Sea at the South Sandwich Trench (Figure 2) or deformed at the Endurance collision zone. The fracture zone azimuths betray large changes in plate divergence direction. These can be expected to have necessitated large changes in ridge-crest orientation to occur by a variety of plate boundary scale processes. The inversion procedure assumes rigid plates and so cannot take these changes into account. I found them to give rise to large populations of data outliers that affected the plausibility of the statistical analysis of the resulting rotation parameters. To combat this problem, I restricted the non-conjugate isochron fits to sets of features with similar strikes.

3. RESULTS

Details of the rotation parameters and their 95% uncertainty ellipsoids are listed in Table 1. Figure 4 gives a visual indication of the goodness of fit and shows that the solution found is acceptable in not implying large changes in spreading direction that are not seen in the fracture zone data. Figure 5 shows the progression of rotation poles, within their 95% confidence ellipses, that broadly follows the West Antarctic coast from west to east before turning southwards. Comparison with the finite rotations of *König and Jokat* (2006) shows the significant additional model constraint that even a modest set of fracture zone data offers.

Figure 6a abstracts the misfits. It can be seen that the standard deviations of the isochron and flowline misfits (22 km and 11 km) are calculated from data populations with even geographical distributions. A prominent group of large isochron misfits is situated in a single spreading corridor in the northeast Weddell Sea on the Antarctic plate. Their confinement to one corridor on one plate suggests a navigational or interpretational error in one or more of the isochrons, or possibly the effects of unidentified spreading asymmetry. The misfits for data in the two segments of ORI do not vary greatly despite being grouped 450 km apart, suggesting that the seaward edges of the Orion-Andenes magnetic anomaly may indeed be an isochron. The large variation in WSE misfits, in contrast, suggests the shape of the modern shelf edge may betray the effects of diachronous continental breakup (*Jokat* et al., 2003) and/or progradation in the east (*Huang* et al., 2014). Neglecting outlier populations, the standard deviations of the isochron and flowline misfit populations are 12 km and 9 km. Data importances (Figure 6b) show that none of the magnetic picks with large misfits has a strong influence on the stability of the solution. The data upon whose alteration the solution would most rapidly change are those in the oldest parts of the Weddell Sea, reflecting above all their scarcity. It can also be seen that the inversion is influenced by, and so has made good use of, a geographically wide spread of the data, meaning it is not unduly biased to any data type or region.

Figure 7 illustrates differences between the model and predictions of the plate circuit (e.g. *Eagles and Vaughan*, 2009). The largest differences are to be seen for times before isochron M11A. Here, flowlines from the two sets of rotations deviate from each other by as much as 120 km, and two magnetic isochrons predicted by the circuit (M22 and M25) are either not present or not resolved in the Weddell Sea. If these deviations were to be interpreted in terms of independent plate motions in the Weddell Sea, then they would imply around 350 km of east-directed convergence somewhere between the Antarctic margins of the Weddell and Riiser Larsen seas in the period before 138 Ma. Neither the size nor the location of this motion is consistent with Cretaceous independent plate motions that have been suggested to the west of the Weddell Sea on the basis of paleomagnetic data (e.g. *Grunow*, 1993; *DiVenere* et al, 1995; *Dalziel and Lawver,* 2001). On the whole, the inversion results depict a smoother plate motion history than the circuit-derived rotations do, consistent with the expectation that spurious accelerations are likely to have been introduced by propagation of errors in the other legs of the circuit. For this reason, I expect errors in the circuit-derived

rotations to be even larger than those shown for the inverse model using 95% confidence ellipses. Taking this into consideration, it seems likely that all of the differences between the two models are products of their combined errors.

4. DISCUSSION: THE ROCAS VERDES BASIN AND PATAGONIAN OROCLINE

It is helpful to date the ORI and WSE rotations in order to relate the history depicted in the model to the development of the Rocas Verdes Basin and Patagonian orocline. Flow points for these rotations bracket the Orion-Andenes magnetic anomaly in the southern Weddell Sea, which *Ferris* et al. (2000) modelled with magnetic susceptibilities in the range reported for seaward-dipping basalt flows associated with continental breakup at the Norwegian margin (*Planke* et al, 1999). WSE may therefore date from the beginning of the Weddell Sea's breakup phase, which can be correlated with the peak of the region's breakup-related Karoo-Ferrar volcanism at 183-177 Ma, or its Chon Aike successor at 172 Ma (Pankhurst et al, 2000). For ORI, I note first that the rotation falls somewhere between those for M25 (~153 Ma) and FIT (183-177 Ma) in the circuit-derived model (Figure 7), and second that a probable sequence of conjugate anomalies to those in the Weddell Sea, formed in the central Scotia Sea, begins around chron M25—M22 (155 Ma; *Eagles*, 2010). ORI should therefore date from a time between 155 and 172-183 Ma. Figure 7 shows that none of the possible combinations of age assignments for ORI and WSE implies unreasonable changes in plate divergence rate or azimuth in the region.

The history of the Rocas Verdes Basin is interpretable from the results of structural and detrital zircon dating work on rocks of its syn- and post-rift fill (e.g. *Calderón* et al., 2007; *Barbeau* et al., 2009; *Gombosi* et al., 2009; *Klepeis* et al., 2010) and U-Pb dating of zircons extracted from igneous rocks of its basement and fill (*Stern* et al., 1992; *Malkowski* et al., 2016). Based on this work, crustal stretching and oceanic crust formation are thought to have occurred in the period 152–141 Ma. The maximum width the basin achieved in this period is not precisely known. *Vérard* et al. (2012) depicted an upper bound of 3000 km by assuming it opened at plate motion rates equal to the fastest currently known. Intercalation of large fan deposits from the basin's opposing margins, however, suggest it was not much wider than 300 km in Tierra del Fuego (*Winn*, 1978). Assuming this width was achieved by stretching of the crust, with factors of between 4 and 5, at the margins of a basaltic floor 100 km wide (*Dalziel*, 1981), the basin there might be attributable to 150—160 km of plate divergence orthogonal to its margins. Further north, where the basin remnants are

narrower, divergence normal to the basin margins is likely to have been slighter. Geochemical indications that the southern reaches of the basin accreted in the presence of a continuous supply of melt from the mantle whilst lavas in the northern reaches were supplied via episodic fractionation support this view (*Stern and de Wit*, 2003). Growth of the Rocas Verdes Basin seems to have ended with its abandonment as a segment of plate boundary around 141 Ma. The basin subsequently filled by deposition of the Yahgan Formation and related rocks. Deformed fossils show that renewed tectonic activity was leading to shortening of the basin by 100 Ma (*Halpern and Rex*, 1972). *Klepeis* et al. (2010) dated undeformed granites that intrude thrust faults to show that this shortening had concluded, at least locally, by 86 Ma.

Figure 8 illustrates some of the plate motions that the model of Table 1 implies to have affected the tectonics of the Rocas Verdes Basin, under the assumption that the East—West Gondwana plate boundary, and later the South America—Antarctica plate boundary, ran at times through the region now occupied by the basin. The base maps show present-day free-air gravity anomalies from *Sandwell* et al. (2014) and *Scheinert* et al. (2016) rotated into their locations at 150 Ma, 140 Ma, 125 Ma and 84 Ma with respect to a fixed East Antarctica. Rotations are from Table 1 (West Gondwana/South America with respect to East Gondwana/Antarctica), *Pérez-Díaz and Eagles* (2014) (Africa with respect to South America) and *Eagles and Jokat* (2014) (for reconstruction of the Scotia Sea). In the following, I describe how the rotations are able to reconstruct a period of basin opening during the time that the East—West Gondwana plate boundary occupied Tierra del Fuego, and a period of oblique basin closure whilst the later South America—Antarctica plate boundary occupied it.

4.1. Closure phase of the Rocas Verdes Basin

Starting around chron MAU (~107 Ma), the directions of modelled relative plate motions rotate anticlockwise through angles of between 60° and 90°, increasing northwestwards. The resulting sense of motion is one of sinistral-oblique shortening throughout the Rocas Verdes Basin (Figure 8a). The obliquity increases southwards where, depending on the specific strike of individual segments of the paleo-plate boundary, even pure strike-slip may have occurred. This is consistent with the findings of *Klepeis* et al. (2010) and *Halpern and Rex* (1972) concerning the timing of the basin's shortening by thrusting and folding, of *Cunningham* (1993; 1995) concerning widespread mid-Cretaceous sinistral oblique and

strike-slip faulting in Tierra del Fuego, of *Olivares* et al. (2003) and *Willner* et al. (2004) concerning sinistral transpression in the margin of the northern parts of the basin, and of the greater width of basin floor remnants in the south than in the north (*Dalziel*, 1981).

The relative plate motion direction during the closure phase is strongly oblique to thrust faults in the internal domain of the Fuegian fold and thrust belt, but less so to the Beagle Channel fault zone (Figure 9). One interpretation of these observations is that mid-Cretaceous strain in the internal zone was partitioned into a convergent component on the thrust faults and a sinistral strike-slip component on the Beagle Channel fault zone. A similar scenario would present the thrusts as developments at bends or step overs between a set of regional strike-slip faults that included lengths of the Beagle Channel and Magallanes-Fagnano fault zones along with at least one further fault zone to the southeast of Beagle Channel. Either possibility would see pervasive non-rigid deformation of the plate boundary zone by movement on faults and shear of the rocks between them. This deformation, which could have involved vertical axis rotations by a variety of mechanisms, is not restored in Figure 8, which accommodates all of the relative plate motion that governed it onto a single narrow plate boundary. Palinspastic restoration of a more realistic wide plate boundary zone, whilst desirable, would require a more complete and reliable data set to describe Cretaceous paleomagnetic rotations and the locations of Cretaceous faults than is available, and so has not be attempted. One of the results of such a restoration would be to reduce the east-west extent of the Fuegian Andes, bringing the region's various occurrences of Cretaceous calc-alkaline and related volcanic rocks (*Hervé* et al., 1984; *Bruce* et al., 1991; *Miller* et al., 1994) closer to the paleo-Pacific subduction zone that *Poblete* et al. (2016) attributed them to.

4.2. Opening phase of the Rocas Verdes Basin

Between chrons WSE and I, the rotations imply orthogonal plate divergence in the region now occupied by the Tortuga complex and oblique-dextral divergence in that now occupied by the Sarmiento complex. The estimated timing of this part of the model overlaps with the 152—141 Ma basin opening phase determined from its fill and floor. If ORI dates to 155 Ma, the model plate divergence implies the basin opened to a width of 140 km orthogonal to its margins in the north, and 280 km in the south during its 152-141 Ma period. Alternatively, if ORI dates to 172 Ma, opening may have been by 65 km in the north and 130 km in the south. These end members bracket the ~160 km estimate of plate divergence made above, and are

also consistent with the geochemical and structural indications that the basin floor became wider and more evolved towards an oceanic composition southwards (*Stern and DeWit*, 2003). The model basin in Figures 8b and 8c, in contrast, appears to widen towards the northwest, because its southern margin has not been palinspastically restored from its post-shortened shape in Figure 8a.

4.3. Quiescent phase of the Rocas Verdes Basin

Figure 8 shows that the Rocas Verdes Basin could have opened by divergence of the East Gondwana and West Gondwana plates until the plate reorganization that led to the fragmentation of West Gondwana, and that it could later have closed by oblique convergence of the South American and Antarctic plates. A remaining question concerns the location of the South America—Antarctica plate boundary in the period between the reorganization near 141 Ma and the start of basin closure after chron MAU (~107 Ma). The boundary's location east of a point on 50°W immediately south of Powell Basin in this period is known from the seafloor spreading evidence in the Weddell Sea (Figure 2). West of this, the only alternative to a South American site is one through what was to become the Antarctic Peninsula, as shown in Figure 8b. Here, the new rotations predict South American–Antarctic convergence after 141 Ma, along an azimuth that *Vaughan* et al. (2012) show is consistent with shortening directions determined from structures in the peninsula's Eastern Palmer Land Shear Zone that they attributed to a collisional event at ~107-103 Ma.

Based on these considerations, it can be stated that major plate motions, initially between East and West Gondwana, led to opening of the Rocas Verdes Basin in extensional and transtensional settings that gave rise to crustal stretching, igneous addition, and oceanization in the period ~152–141 Ma. Abandonment of the basin around 141 Ma, possibly one of a number of regional consequences of the changing stress field related to the breakup of West Gondwana by initiation of the southern Mid Atlantic Ridge, resulted in the transfer of a strip of lithosphere from the western margin of the inactive basin to the new South American plate. The crust of this strip consisted of pre-early Cretaceous basement of the Patagonian Andes and, at least by a short while prior to the Palmer Land Event at 107-103 Ma, the western and central terranes of the Antarctic Peninsula. As shown by *Vaughan* et al. (2012), relative plate motion between these terranes and the interior of Antarctica was convergent, leading to their eventual collision. Following collision, a further

relocation of the plate boundary to southern Tierra del Fuego saw it come to accommodate oblique plate convergence to close the Rocas Verdes Basin.

4.4. Oblique convergence and the curvature of the Patagonian Orocline

Figures 8 and 9 demonstrate how major plate motions alone are able to explain the timing, sense, orientation and magnitude of the opening and closure of the Rocas Verdes Basin. The closure of the Rocas Verdes Basin in this model occurs about stage poles in equatorial latitudes, at which distance large local rotations of the plate on the Pacific side of the basin are impossible. The idea of the basin closing and the Fuegian Andes bending by motion of a small plate driven by forces raised at its Pacific margin reduces to an *ad hoc* explanation for the apparent vertical-axis rotations of the region's Cretaceous rocks. The strong obliquity of plate motion beginning during the closure phase is, in contrast, fully consistent with *Cunningham's* (1993; 1995) representation of the orocline and its paleomagnetic rotations as plate boundary and crustal-scale products of Cretaceous through to Paleogene strike-slip related processes. As this is envisaged to have occurred by what, at the plate scale, amounts to distributed deformation (*Garfunkel and Ron*, 1985), it would not be appropriate in Figure 8 to depict it using rotations of rigid lithospheric blocks like those of *Poblete* et al. (2015).

The obliquity of plate motion during the Cretaceous closure phase to the present-day strikes of thrust faults in the internal domain of the Fuegian fold and thrust belt varies in the range 15°-30° (Figure 9). At such obliquities, reduction of a 100 km wide basaltic basin floor to the present-day 15 km outcrop width of the Tortuga ophiolite would require between 330 km and 170 km of oblique plate convergence. Starting immediately after the Palmer Land deformation, the model in Table 1 would achieve these values by 77 Ma or 91 Ma, which can be seen as consistent with *Klepeis* et al.'s (2010) 86 Ma date for the end of thrusting in the Rocas Verdes Basin. Either of these amounts of convergence alone, however, would be insufficient to explain the ~400 km length of the east-striking limb of the Patagonian orocline as a product of deformation of an originally rectilinear margin. The rotations in Table 1, however, imply continuing oblique sinistral convergence well into Paleogene times (Figure 9). Numerous studies present evidence for this convergence, as well as for vertical axis rotations (e.g. *Nelson*, 1982; *Cunningham*, 1995; *Gombosi* et al., 2009; *Poblete* et al., 2016; Figure 1). Although this later activity seems primarily to have affected the area to the north of the Beagle Channel fault zone, *Barbeau* et al. (2009) give evidence, albeit whose significance they questioned as possibly a consequence of sample contamination, from a

small population of zircons for its ongoing tectonics into the period 83-75 Ma. Conceivably, therefore, the present-day curvature of the southernmost Andes is entirely a consequence of mid-Cretaceous to Paleogene oblique convergence within the South American-Antarctic plate boundary zone.

5. CONCLUSIONS

I have used Euler rotations derived from a new model of seafloor spreading data in the Weddell Sea to show that Cretaceous tectonics within the Andean margin of southwest Gondwana was determined at first order by relative plate motions caused by fragmentation of the supercontinent. This conclusion can be independently supported by existing paleomagnetic and structural geological data that show the Patagonian orocline formed during mid Cretaceous to Paleogene deformation and rotation of upper crustal rocks between regional strike-slip and thrust faults in the margins and the floor of a narrow latest-Jurassic to early Cretaceous oceanic basin that ran through Tierra del Fuego from the Pacific to the Weddell Sea.

ACKNOWLEDGEMENTS

I acknowledge the Alfred Wegener Institute, Helmholtz Centre for Polar and Marine Research, for funding this work. Figures were created with the Generic Mapping Tools. Dickson Cunningham and Lucía Pérez Díaz read and commented on the manuscript. I thank Fernando Poblete and an anonymous reviewer for their constructive comments on the manuscript.

REFERENCES

[1] Arctowski H, 1895, Observations sur l'interet qui presente l'exploration des Terres Australes. *Bull Soc Geol Fr (ser 3)*, 23, 589–591.

[2] Barbeau, D. L. Jr., Gombosi, D.J., Zahid, K.M., Bizimis, M., Swanson-Hysell, N., Valencia, V., and Gehrels, G.E., 2009, U-Pb zircon constraints on the age and provenance of the Rocas Verdes basin fill, Tierra del Fuego, Argentina, *Geochem. Geophys. Geosyst.*, 10, Q12001, doi:10.1029/2009GC002749

[3] Barker, P.F. and Jahn, R.A. 1980. A marine geophysical reconnaissance of the Weddell Sea. *Geophys. J. Roy. Astr. Soc.* 63, 271–283.

[4] Barker, P.F., Barber, P.L., and King, E.C., 1984, An early Miocene ridge crest–trench collision on the South Scotia Ridge near 36°W, *Tectonophysics*, 102, 315-332.

[5] Betka, P., Klepeis, K. and Mosher, S., 2016. Fault kinematics of the Magallanes-Fagnano fault system, southern Chile; an example of diffuse strain and sinistral transtension along a continental transform margin. *Journal of Structural Geology*, *85*, 130-153.

[6] Bruce, R.M., Nelson, E.P., Weaver, S.G. and Lux, D.R., 1991. Temporal and spatial variations in the southern Patagonian batholith; Constraints on magmatic arc development. *Geological Society of America Special Papers*, *265*, 1-12.

[7] Carey, W.S., 1955, The orocline concept in geotectonics-Part I, In *Papers and proceedings of the Royal Society of Tasmania*, 89, 255-288.
[8] Cunningham, W.D., Klepeis, K.A., Gose, W.A., Dalziel, I.W.D., 1991. The Patagonian Orocline: new paleomagnetic data from the Andean Magmatic Arc in Tierra del Fuego, Chile. J. Geophys. Res. 96 (B10), 16061–16067. http://dx.doi.org/10.1029/ 91jb01498.
[9] Cunningham, W.D., 1993, Strike- slip faults in the southernmost Andes and the development of the Patagonian orocline. *Tectonics*, *12*, 169-186.
[10] Cunningham, W.D., 1995, Orogenesis at the southern tip of the Americas: the structural evolution of the Cordillera Darwin metamorphic complex, southernmost Chile. *Tectonophysics*, *244*, 197-229.
[11] Dalziel I. W. D., 1981, Back-arc extension in the southern Andes: a review and critical reappraisal. *Phil. Trans. R. Soc. London* A300*:* 319–335.
[12] Dalziel, I.W.D. and Lawver, L.A., 2001. The lithospheric setting of the West Antarctic ice sheet. *The West Antarctic Ice Sheet: Behavior and Environment, Antarct. Res. Ser*, *77*, 29-44.
[13] Dalziel, I.W., Lawver, L.A., Norton, I.O. and Gahagan, L.M., 2013. The Scotia Arc: genesis, evolution, global significance. *Ann. Rev. Ear. Plan. Sci.*, *41*, 767-793.
[14] DeMets, C., Gordon, R.G. and Argus, D.F., 2010. Geologically current plate motions. *Geophys. J. Int.*, *181*, 1-80.
[15] DiVenere, V., Kent, D.V., and Dalziel, I.W.D., 1995, Early Cretaceous paleomagnetic results from Marie Byrd Land, West Antarctica: Implications for the Weddellia collage of crustal blocks, *J. Geophys. Res*., 100, 8133-8151.
[16] Eagles, G., 2005, Tectonic evolution of the west Scotia Sea, *J. Geophys. Res*., 110, B02401, doi:10.1029/2004JB003154.
[17] Eagles, G. and Vaughan, A.P., 2009. Gondwana breakup and plate kinematics: business as usual, *Geophys. Res. Lett.*, *36*(10).
[18] Eagles, G., Age and origin of the central Scotia Sea, 2010b, *Geophys. J. Int.*, 183, 587-600, doi: 10.1111/j.1365-246X.2010.04781.x
[19] Eagles, G. and Jokat, W., 2014. Tectonic reconstructions for paleobathymetry in Drake Passage. *Tectonophysics*, *611*, 28-50.
[20] Ferris, J.K., Vaughan, A.P.M., and Storey, B.C., 2000, Relics of a complex triple junction in the Weddell Sea Embayment, Antarctica, *Earth Planet. Sci. Lett.*, 178, 215-230.
[21] Freund, R., 1974, Kinematics of transform and transcurrent faults, *Tectonophysics*, 21, 93-134.
[22] Garfunkel, Z., and Ron, H., Block rotation and deformation by strike-slip faults 2. The properties of a type of macroscopic deformation, *J. Geophys. Res*., 90, 8589-8602.
[23] Ghidella, M.E., G. Yáñez, and J.L. LaBrecque, 2002, Revised tectonic implications for the magnetic anomalies of the western Weddell Sea, *Tectonophysics*, 347, 65-86.
[24] Ghiglione, M.C. and Cristallini, E.O., 2007. Have the southernmost Andes been curved since Late Cretaceous time? An analog test for the Patagonian Orocline. *Geology*, *35*, 13-16.
[25] Granot, R., Dyment, J., and Gallet, Y., 2012, Geomagnetic field variability during the Cretaceous Normal Superchron, *Nature Geoscience*, 5, 220-223, doi:10.1038/ngeo1404
[26] Golynsky, A.V., Morris, P., von Frese, R., and the ADMAP group, 2001, *ADMAP – Magnetic anomaly map of the Antarctic*, 1:10000000 scale map, BAS (Misc) 10, Cambridge, British Antarctic Survey.
[27] Gombosi, D.J., Barbeau Jr, D.L. and Garver, J.I., 2009, New thermochronometric constraints on the rapid Palaeogene exhumation of the Cordillera Darwin complex and related thrust sheets in the Fuegian Andes. *Terra Nova*, *21*, 507-515.
[28] Grunow, A.M., 1993, The creation and destruction of Weddell Sea floor in the Jurassic, *Geology*, 21, 647-650.
[29] Halpern, M., and D. C. Rex, 1972, Time of folding of the Yahgán Formation and age of the Tekenika Beds, southern Chile, and South America. *Geol. Soc. Am. Bull., 83*, 1881-1886.
[30] Hervé, M., Suárez, M., and Puig, A., 1984, The Patagonian batholith S of Tierra del Fuego, Chile: timing and tectonic implications, *J. Geol. Soc. London*, 141, 909-917.
[31] Huang, X., Gohl, K. and Jokat, W., 2014. Variability in Cenozoic sedimentation and paleo-water depths of the Weddell Sea basin related to pre-glacial and glacial conditions of Antarctica. *Global Planet. Change*, *118*, 25-41.

[32] Jokat, W., Boebel, T., König, M. and Meyer, U., 2003, Timing and geometry of early Gondwana breakup, *J. Geophys. Res.*, 108, 2428, doi:10.1029/2002JB001802.
[33] Klepeis, K.A., 1994b. The Magallanes and Deseado fault zones; major segments of South American-Scotia transform plate boundary in southernmost South America, Tierra del Fuego. *J. Geophys. Res*. 99, 22.
[34] Klepeis, K.A., Austin, J., 1997. Contrasting styles of superposed deformation in the southernmost andes. Tectonics 16, 776e755.
[35] Klepeis, K., P. Betka, G. Clarke, M. Fanning, F. Hervé, L. Rojas, C. Mpodozis, and S. Thomson, 2010, Continental underthrusting and obduction during the Cretaceous closure of the Rocas Verdes rift basin, Cordillera Darwin, Patagonian Andes, *Tectonics*, 29, TC3014, doi:10.1029/2009TC002610.
[36] König, M. and Jokat, W., 2006, The Mesozoic breakup of the Weddell Sea, *J. Geophys. Res.*. 111, B12102, doi:10.1029/2005JB004035.
[37] Kraemer, P.E., 2003. Orogenic shortening and the origin of the Patagonian orocline (56 S. Lat). *J. S. Am. Earth Sci.*, *15*, 731-748.
[38] LaBrecque, J.L. and Barker, P.F. 1981. The age of the Weddell Basin, *Nature,* 290, 489-492
[39] Livermore, R. and Hunter, R., 1996, Mesozoic seafloor spreading in the Southern Weddell Sea. In Storey, B.C., King, E.C. & Livermore, R.A. (eds.): *Weddell Sea Tectonics and Gondwana Break-up, Geol. Soc. Spec. Publ*., 108, 227-241.
[40] Livermore, R. and Woollett, R., 1993, Seafloor spreading in the Weddell Sea and Southwest Atlantic since the Late Cretaceous. *Earth Planet. Sci. Lett.*, 117, 475-495.
[41] Livermore, R. A., Nankivell, A., Eagles, G., and Morris, P., 2005, Paleogene opening of Drake Passage, *Earth. Planet. Sci. Lett.,* 236, 459-470.
[42] Lodolo, E., Menichetti, M., Bartole, R., Ben-Avraham, Z., Tassone, A., Lippai, H., 2003. Magallanes-Fagnano continental transform fault (Tierra del Fuego, southernmost South America). *Tectonics*, 22, 1076. http://dx.doi.org/10.1029/ 2003TC001500.
[43] Malkowski, M.A., Grove, M., and Graham, S.A., 2016, Unzipping the Patagonian Andes—Long-lived influence of rifting history on foreland basin evolution, Lithosphere, 8, 23-28.
[44] Marshak, S., 1988. Kinematics of orocline and arc formation in thin- skinned orogens. *Tectonics*, *7*(1), 73-86.
[45] Menard, H.W., 1978. Fragmentation of the Farallon plate by pivoting subduction. *J. Geol.*, 86, 99-110.
[46] Menichetti, M., Lodolo, E., Tassone, A., 2008. Structural geology of the Fuegian Andes and Magallanes fold-and-thrust belt - Tierra del Fuego Island. Geol. Acta 6, 19-42.
[47] Miller, C.A., Barton, M., Hanson, R.E. and Fleming, T.H., 1994. An Early Cretaceous volcanic arc/marginal basin transition zone, Peninsula Hardy, southernmost Chile. *Journal of volcanology and geothermal research*, *63*, 33-58.
[48] Nelson, E.P., 1982, Post-tectonic uplift of the Cordillera Darwin orogenic core complex: evidence from fission track geochronology and closing temperature—time relationships, *J. Geol. Soc. Lond*., 139, 755—761.
[49] Olivares, B., Cembrano, J., Hervé, F., López, G., and Prior, D., 2003, Geometría y cinemática de la Zone de Cizalle Seno Arcabuz, Andes patagónicos, Chile, *Rev. geol. Chile*, 30, 39—52.
[50] Pankhurst, R.J., Riley, T.R., Fanning, C.M. and Kelley, S.P., 2000. Episodic silicic volcanism in Patagonia and the Antarctic Peninsula: chronology of magmatism associated with the break-up of Gondwana. *J. Petrology*, *41*, 605-625.
[51] Pérez-Díaz, L., and Eagles, G., 2014, Constraining South Atlantic growth with seafloor spreading data, *Tectonics*, 33, doi:10.1002/2014TC003644
[52] Planke, S., Cerney, B., Bücker, C.J. & Nilsen, O., 1999, Alteration effects on petrophysical properties of subaerial flood basalts: Site 990, Southeast Greenland margin. *In:* Larsen, H.C., Duncan, R.A., Allen, J.F. & Brooks, K. (eds) *Proceedings of the Ocean Drilling Program Scientific Results 163*. Ocean Drilling Program, College Station, TX, 17–28.
[53] Poblete, F., Roperch, P., Hervé, F., Diraison, M., Espinoza, M. and Arriagada, C., 2014. The curved Magallanes fold and thrust belt: Tectonic insights from a paleomagnetic and anisotropy of magnetic susceptibility study. *Tectonics*, *33*, 2526-2551.

[54] Poblete, F., Roperch, P., Arriagada, C., Ruffet, G., de Arellano, C.R., Hervé, F. and Poujol, M., 2016. Late Cretaceous–early Eocene counterclockwise rotation of the Fueguian Andes and evolution of the Patagonia–Antarctic Peninsula system. *Tectonophysics*, 668-669, 15-34.

[55] Rapalini, A.E., Peroni, J., Luppo, T., Tassone, A., Cerredo, M.E., Esteban, F., Lippai, H., Franciscovilas, J., 2015. Palaeomagnetism of Mesozoic magmatic bodies of the Fuegian Cordillera: implications for the formation of the Patagonian Orocline. *Geol. Soc. Spec. Publ*. http://dx.doi.org/10.1144/sp425.3.

[56] Ron, H., Freund, R., Garfunkel, Z., and Nur, A., 1984, Block rotation by strike-slip faulting: structural and paleomagnetic evidence, *J. Geophys. Res*., 89, 6256—6270.

[57] Sandwell, D.T., Müller, R.D., Smith, W.H., Garcia, E. and Francis, R., 2014. New global marine gravity model from CryoSat-2 and Jason-1 reveals buried tectonic structure. *Science*, *346,* 65-67.

[58] Scheinert, M., Ferraccioli, F., Schwabe, J., Bell, R., Studinger, M., Damaske, D., Jokat, W., Aleshkova, N., Jordan, T., Leitchenkov, G., Blankenship, D.D., Damiani, T.M., Young, D., Cochran, J.R., and Richter, T.D., 2016. New Antarctic gravity anomaly grid for enhanced geodetic and geophysical studies in Antarctica. *Geophys. Res. Lett.*, 43, doi:10.002/2015GL067439.

[59] Somoza, R., and Zaffarana, C.B., 2008, Mid-Cretaceous polar standstill of South America, motion of the Atlantic hotspots and the birth of the Andean cordillera, *Earth Planet. Sci.* Lett., 271, 267—277.

[60] Stern, C.R. and Mukasa, S.B., 1992, Age and petrogenesis of the Sarmiento ophiolite complex of southern Chile, *Journal of South American Earth Sciences*, *6*, 97-104.

[61] Stern, C.R. and De Wit, M.J., 2003. Rocas Verdes ophiolites, southernmost South America: remnants of progressive stages of development of oceanic-type crust in a continental margin back-arc basin. *Geol. Soc., Lond. Spec. Publ.*, *218*, 665-683.

[62] Sue, C., and Ghiglione, M., 2016, Wrenching tectonism in the Southernmost Andes and the Scotia Sea constrained from fault kinematic and seismotectonic overviews, in: *Geodynamic Evolution of the southernmost Andes: Connections with the Scotia Arc*, Ghiglione, M., ed., Springer. doi:10.1007/978-3-319-39727-6

[63] Torres Carbonell, P.J., Olivero, E.B., and Dimieri, L.V., 2008, Structure and evolution of the Fuegian Andes foreland thrust-fold belt, Tierra del Fuego, Argentina: paleogeographic implications, *J. S. Am. Earth Sci.*, 25, 417-439

[64] Torres Carbonell, P.J., Dimieri, L.V., Olivero, E.B., Bohoyo, F. and Galindo-Zaldívar, J., 2014. Structure and tectonic evolution of the Fuegian Andes (southernmost South America) in the framework of the Scotia Arc development. *Global and Planetary Change*, *123*, 174-188.

[65] Torres Carbonell, P.J., Guzmán, C., Yagupsky, D. and Dimieri, L.V., 2016. Tectonic models for the Patagonian orogenic curve (southernmost Andes): An appraisal based on analog experiments from the fuegian thrust-fold belt. *Tectonophysics*, 671, 76-94.

[66] Vaughan, A.P.M., Eagles, G., and Flowerdew, M.J., 2012, Evidence for a two-phase Palmer Land event from cross-cutting structural relationships and emplacement timing of the Lassiter Coast Intrusive Suite, Antarctic Peninsula: Implications for mid-Cretaceous Southern Ocean plate configuration. *Tectonics*, 31(1), doi:10.1029/2011TC003006.

[67] Vérard, C., Flores, K., and Stampfli, G., 2011, Geodynamic Reconstructions of the South America–Antarctica Plate System, *J. Geodyn.*, 53, 43-60.

[68] Willner, A.P., Hervé, F., Thomson, S.N., and Massone, H.-J., 2004, Converging P-T paths of Mesozoic HP-LT metamorphic units (Diego de Almagro Island, Southern Chile): evidence for juxtaposition during late shortening of an active continental margin, Mineralogy and Petrology, 81, 43-84.

[69] Winn, R. D., 1978, Upper Mesozoic flysch of Tierra del Fuego and South Georgia Island. A sedimentologic approach to lithosphere restoration. *Geol. Soc. Am. Bull. 89*, 533-547.

FIGURES

Figure 1. a) The Patagonian orocline as defined primarily by anomalous paleomagnetic rotations (discs coded by colour for age, grey wedges portray the anomalies as deviations from present-day north; after *Poblete* et al., 2014; 2016), including rocks of the Rocas Verdes Basin (green shades; including the Sarmiento (SC) and Tortuga (TC) ophiolite complexes) and Jurassic-Paleogene batholith at its Pacific margin. Red lines: regional scale oblique- and strike-slip fault zones after Sue and Ghiglione (2016) including BF: Beagle Channel fault zone; MF: Magallanes-Fagnano fault zone; b) schematic of orocline formation from an originally rectilinear Pacific margin of Gondwana by action and evolution of strike-slip (green), transpressional (red) and transtensional (blue) faults in the plate boundary zone between the South American and Antarctic plates at the northern end of the Antarctic Peninsula (ANP) (adapted from *Cunningham*, 1993), c) schematic of orocline formation by plate rotations (after *Poblete* et al., 2016). Yellow: African plate, Blue: South American plate, Green: Antarctic plate; Red: 'Rocas Verdes' plate bearing the rocks that today exhibit anomalous paleomagnetic rotations (hatched pattern).

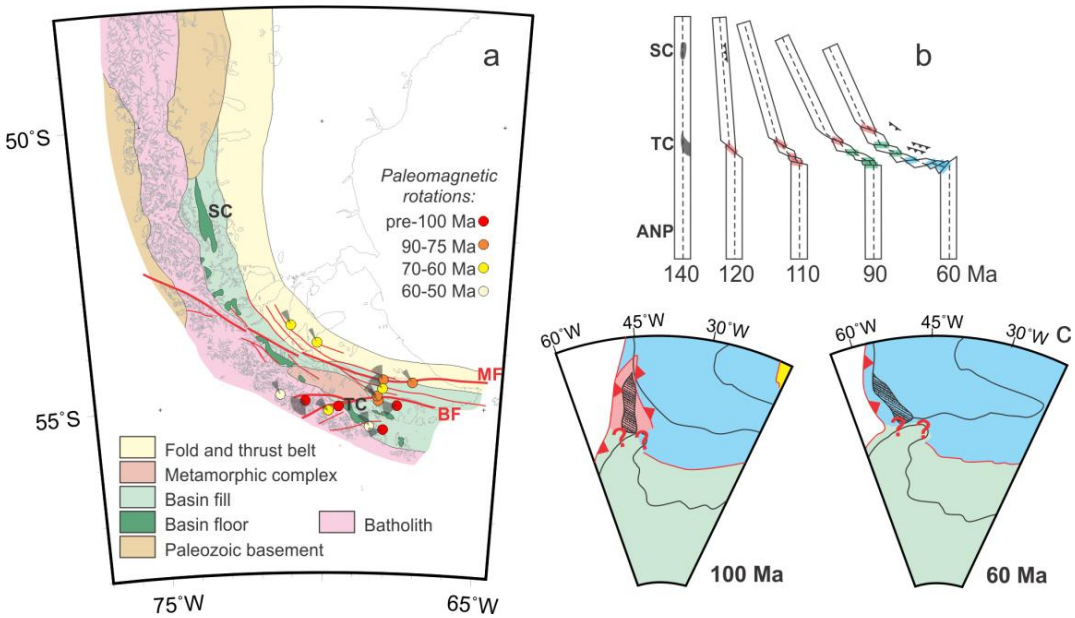

Figure 2. The Weddell Sea. a: Satellite-derived gravity data (*Sandwell* et al., 2014 and *Scheinert* et al., 2016 on land in Antarctica). T: anomaly T. Black triangles: FZ picks. MAU: picks at rifted edge of Maud Rise. WSE: picks at edge of Weddell Sea continental shelf. Yellow fill area with 'Sur' label: area in which seafloor may have been affected by independent motion of Sur component plate. b: trackline data compiled or acquired by AWI (red), ADMAP (blue), and BAS (black). Thick red lines: triple junction traces, dashed red lines: other margins of the region formed by seafloor spreading in the Weddell Sea. Symbols locate magnetic reversal isochron picks made in the trackline data.

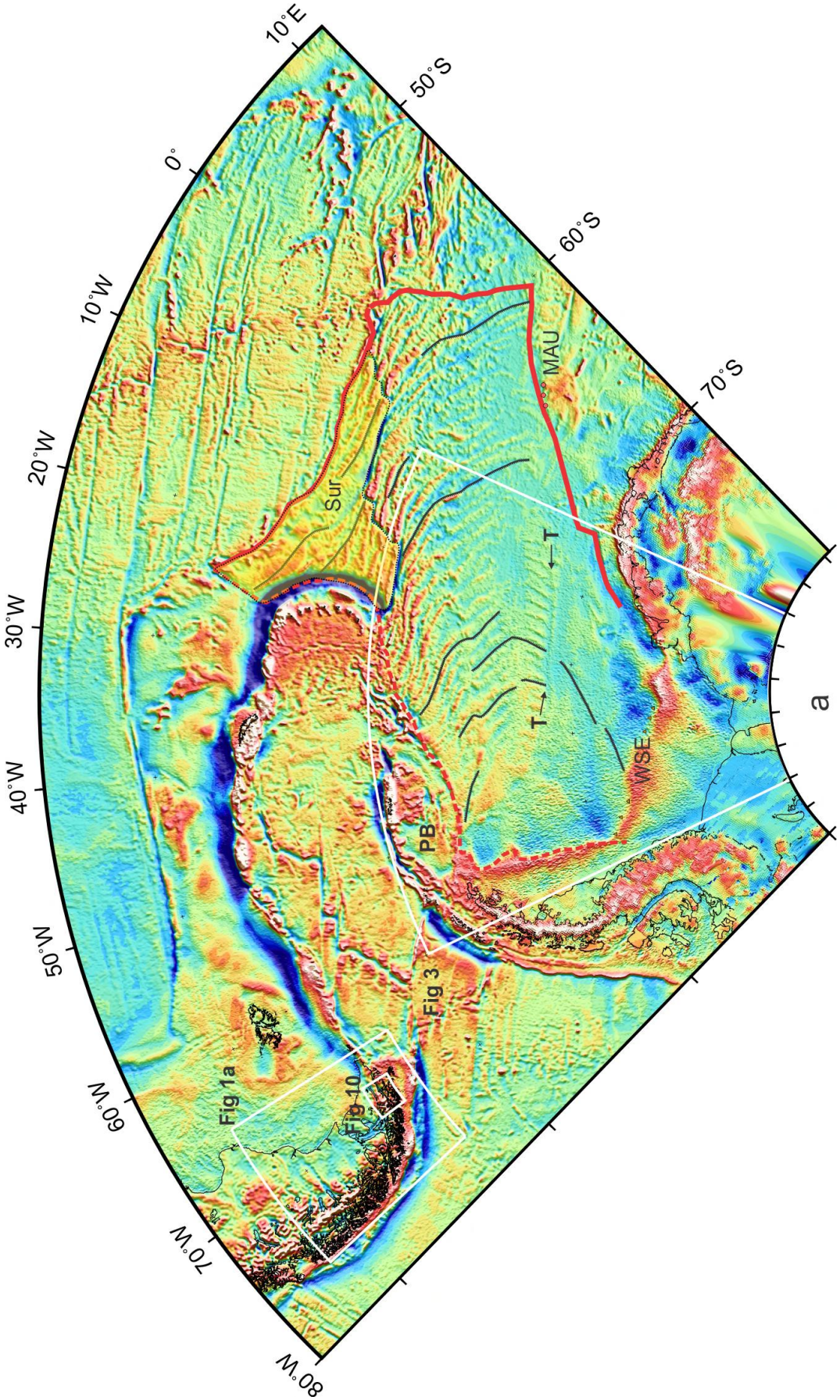
10°E
0°
10°W
20°W
30°W
40°W
50°W
60°W
70°W
80°W
50°S
60°S
70°S
Sur
MAU
T
T
WSE
PB
Fig 3
Fig 1a
Fig 10
a

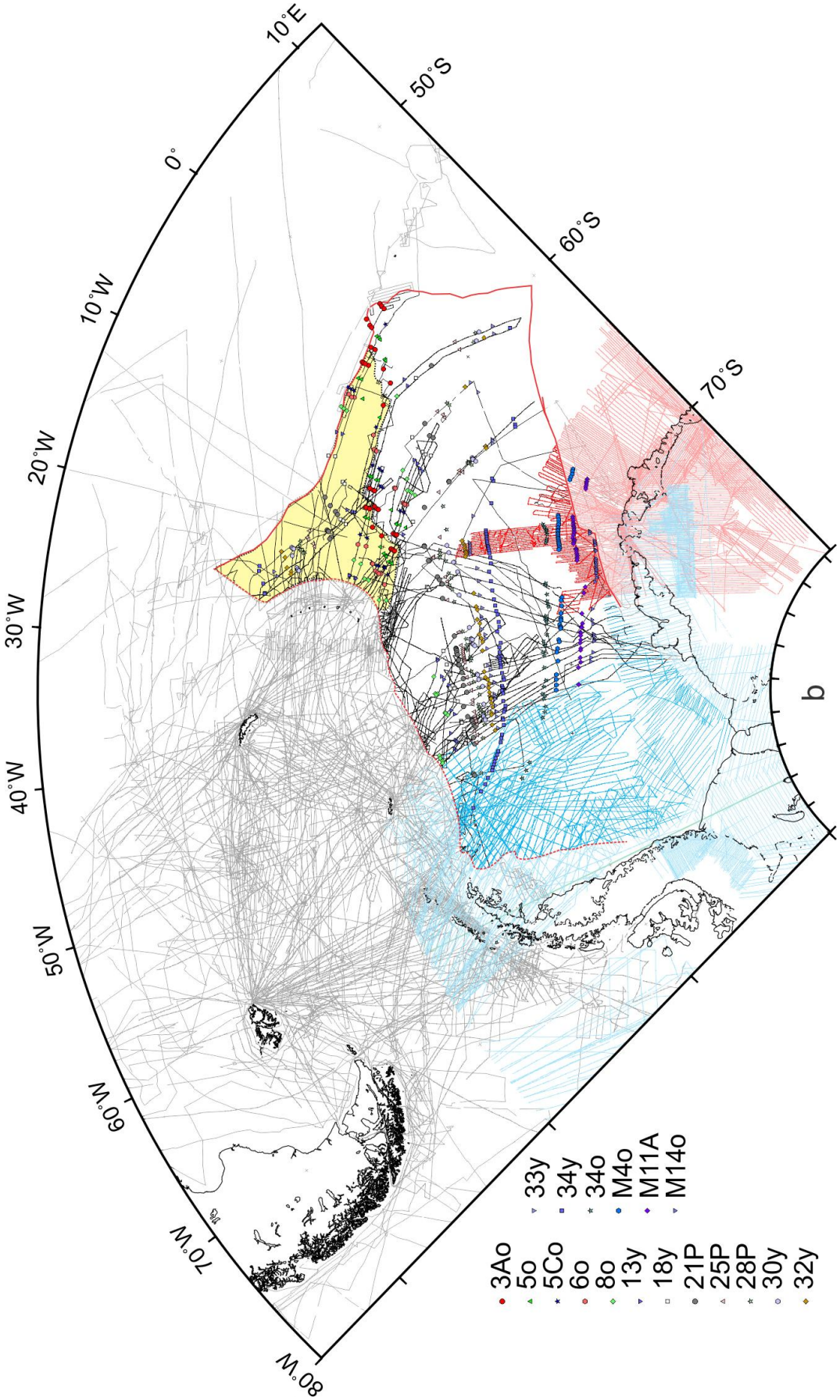
10°E
0°
10°W
20°W
30°W
40°W
50°W
60°W
70°W
80°W
50°S
60°S
70°S
b
3Ao
5o
5Co
6o
8o
13y
18y
21P
25P
28P
30y
32y
33y
34y
34o
M4o
M11A
M14o

Figure 3. Magnetic grid from ADMAP compilation (*Golynsky* et al, 2001) with grid-based picks of isochrons I, I2 and ORI. O-A Anomaly: Orion-Andenes Anomaly.

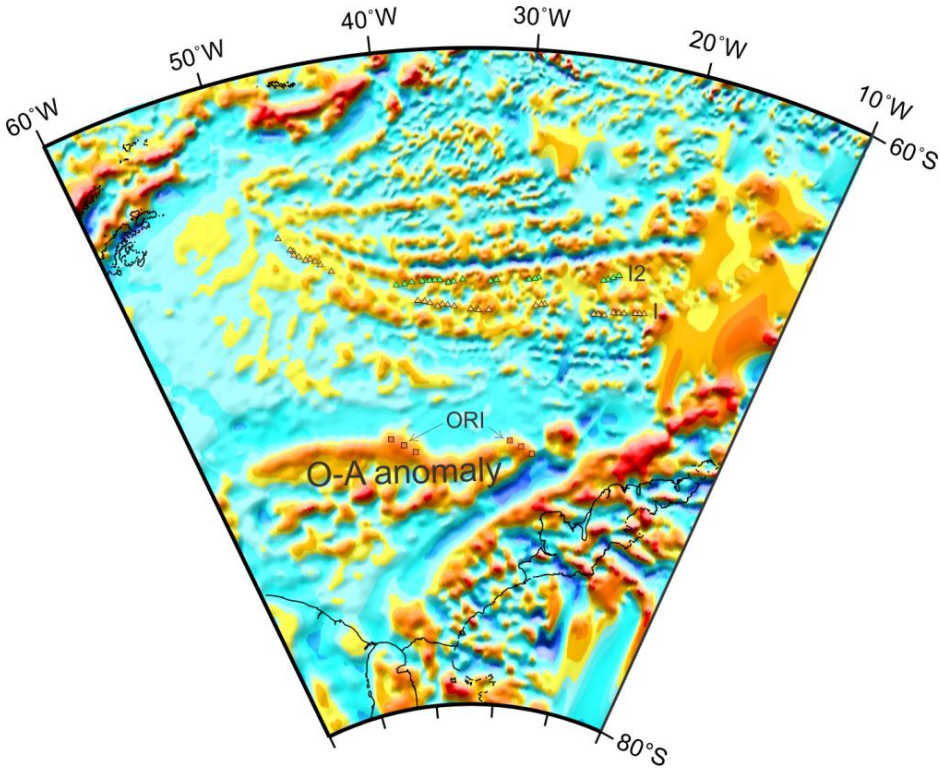

Figure 4. Visual fits in inversion elements. Blue lines: Synthetic flowlines.

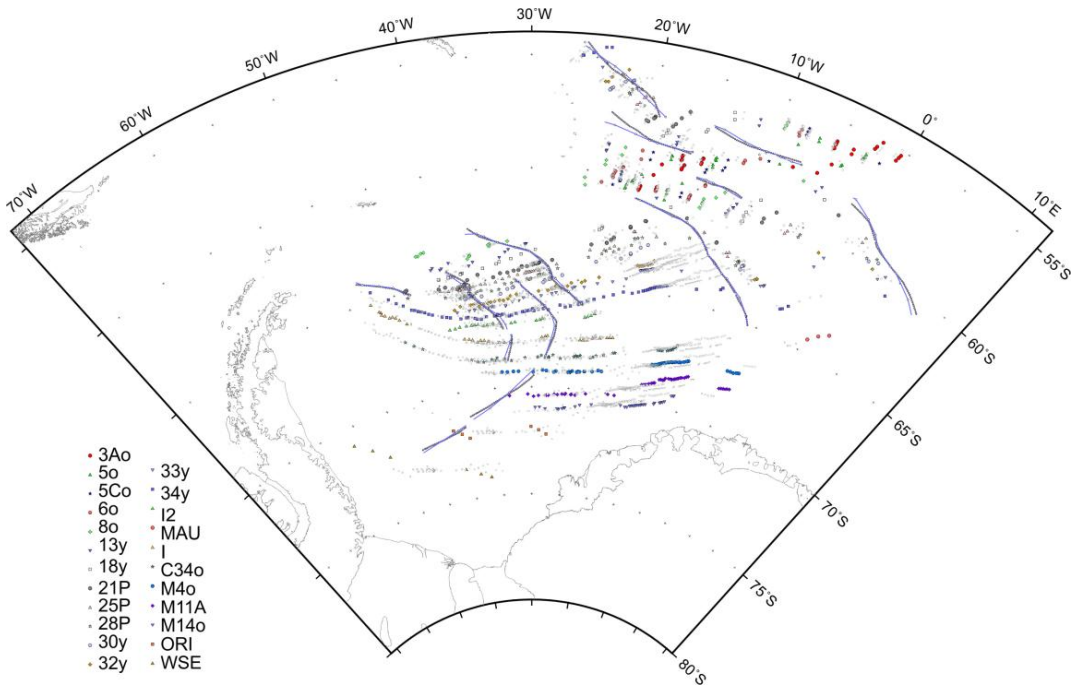

Figure 5. Finite rotation poles and their 95% confidence ellipses for motion of Antarctica with respect to South America. Red: this study, Blue: *König and Jokat*, 2006; Green: *Eagles and Vaughan*, 2009.

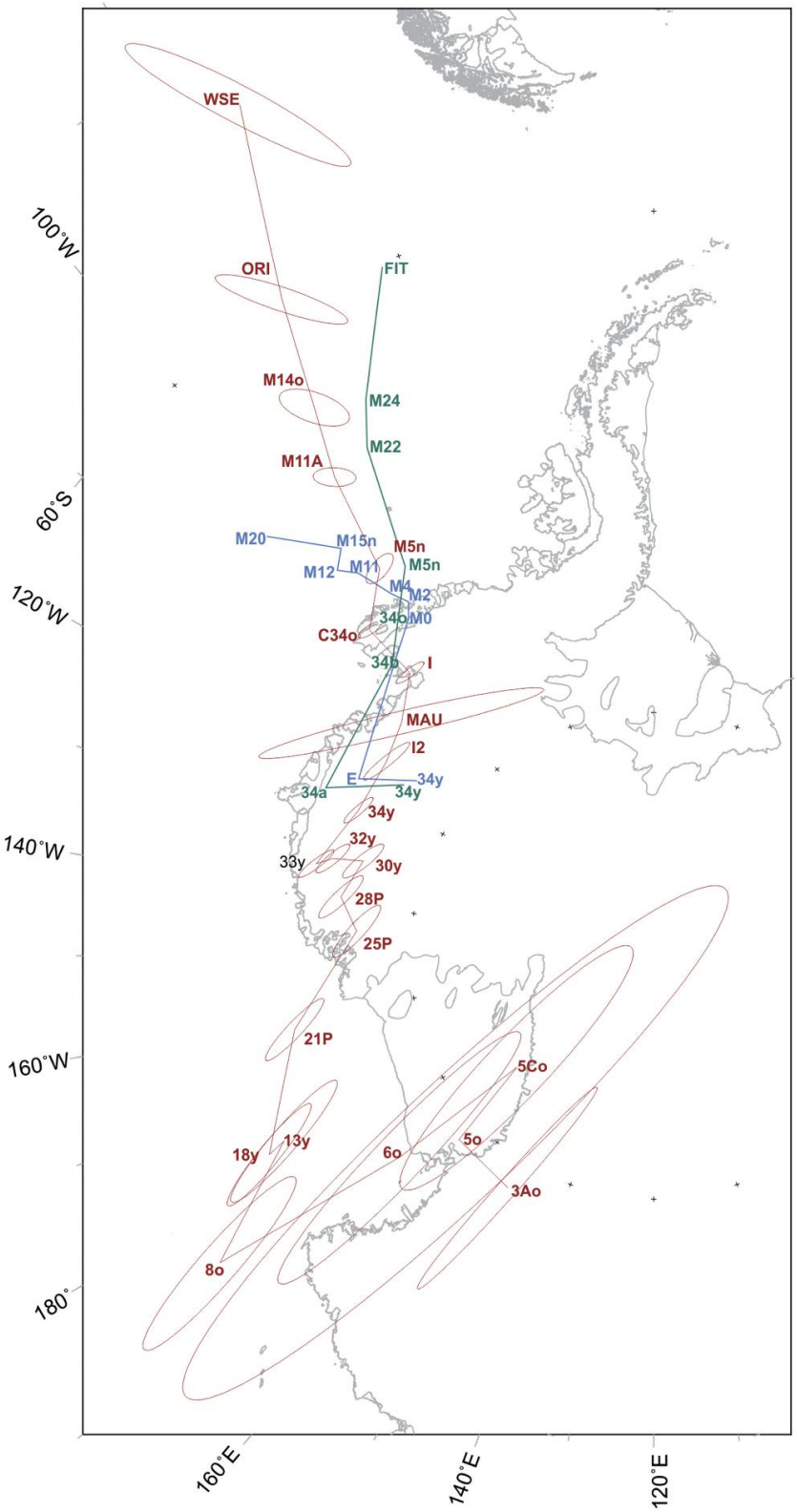

Figure 6. a) Model misfits to the data. Blue: RMS misfits to isochron data. Pink: misfits to fracture zone data. b) Data importances to the stability of the model. Dark green: importance of isochron data point. Light green: importance of fracture zone data point.

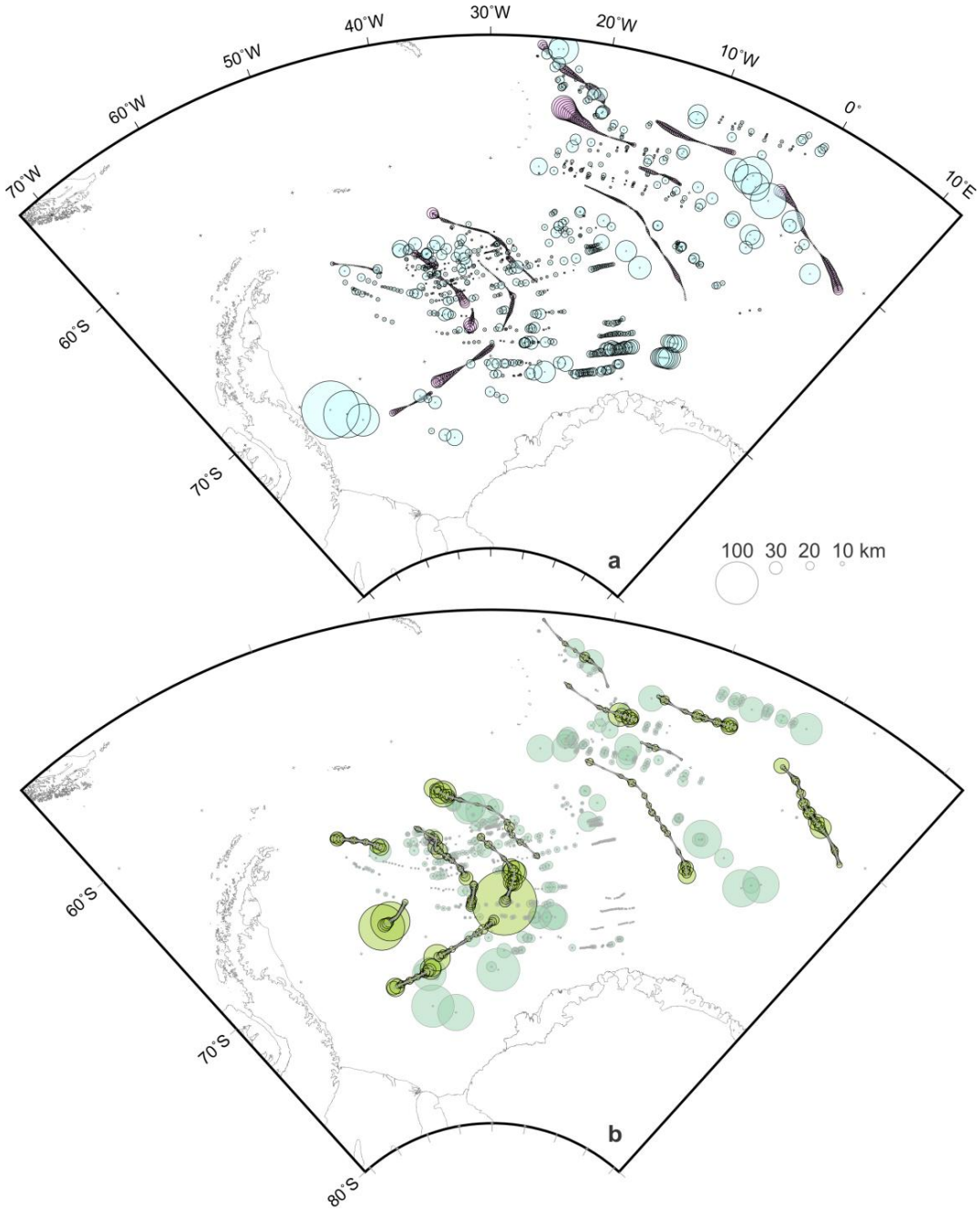

Figure 7. Comparison of model flowlines generated from the South America-Africa-Antarctic plate circuit (blue) and inversion (red) methods. Top upper inset: older parts of the models showing expected locations of flowpoints for chrons M25 and M22 assuming for the inverse model that steady plate divergence rates and that ORI dates to 157.5 Ma, Bottom upper inset: same, assuming instead that ORI dates from 172 Ma. Lower inset: plate divergence rates (red shades) and azimuths (blue shades) along the flowlines shown, as implied by variable models and age assignments to ORI and WSE. Plain lines: ORI at 157 Ma and WSE at 172 Ma; long dashes: ORI at 172 Ma and WSE at 183 Ma; short dashes: ORI at 157 Ma and WSE at 183 Ma. Bold lines: circuit-derived model (Eagles and Vaughan, 2009).

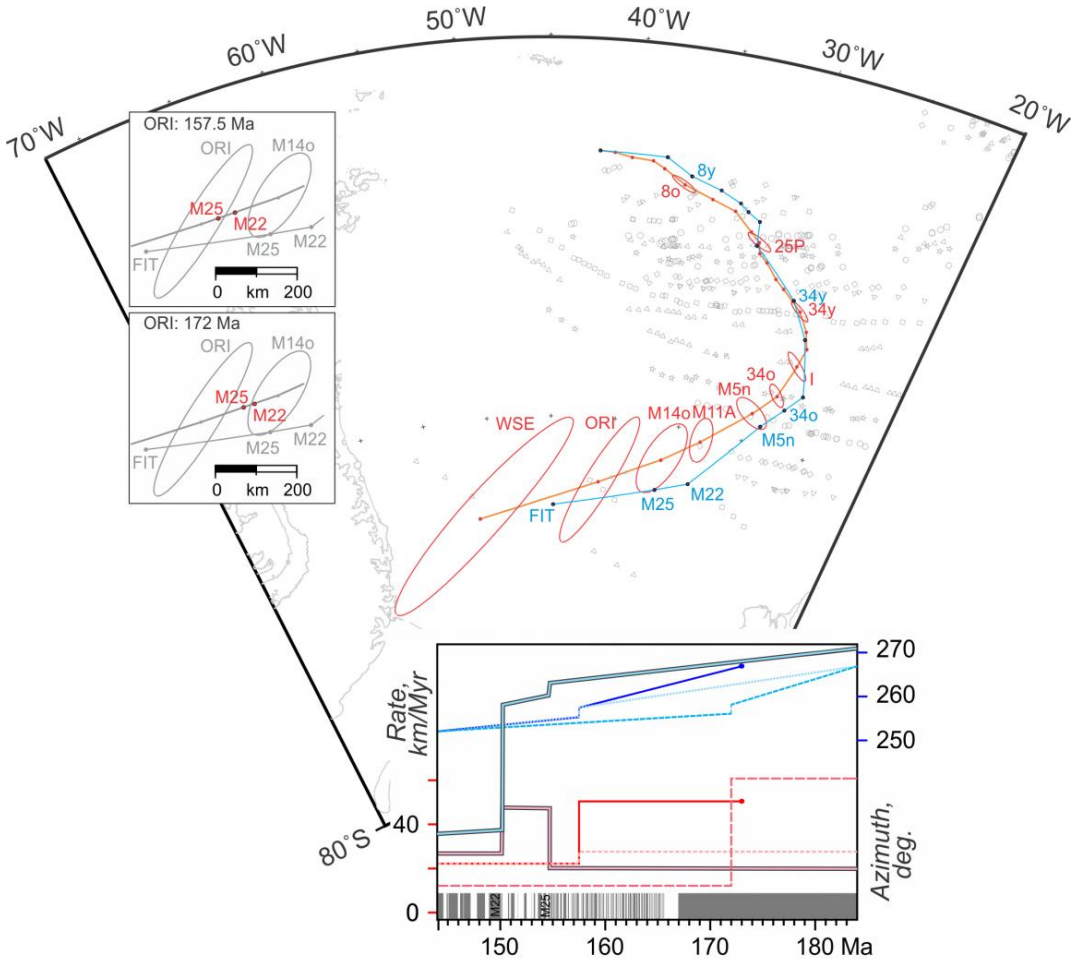

Figure 8. Possible history of activation and inversion of the Rocas Verdes Basin by plate boundary switching. a,b: Basin opening phase by divergent motion (blue vectors, for 150-140 Ma) of West and East Gondwana; c: Quiescent phase after basin abandonment during plate boundary reorganization; d: closure phase by oblique sinistral motion between South American (SAM) and Antarctic (ANT) plates (vectors for 94-84 Ma). AFR: African plate. Green: present-day Rocas Verdes ophiolite outcrops (from *Klepeis* et al., 2010).

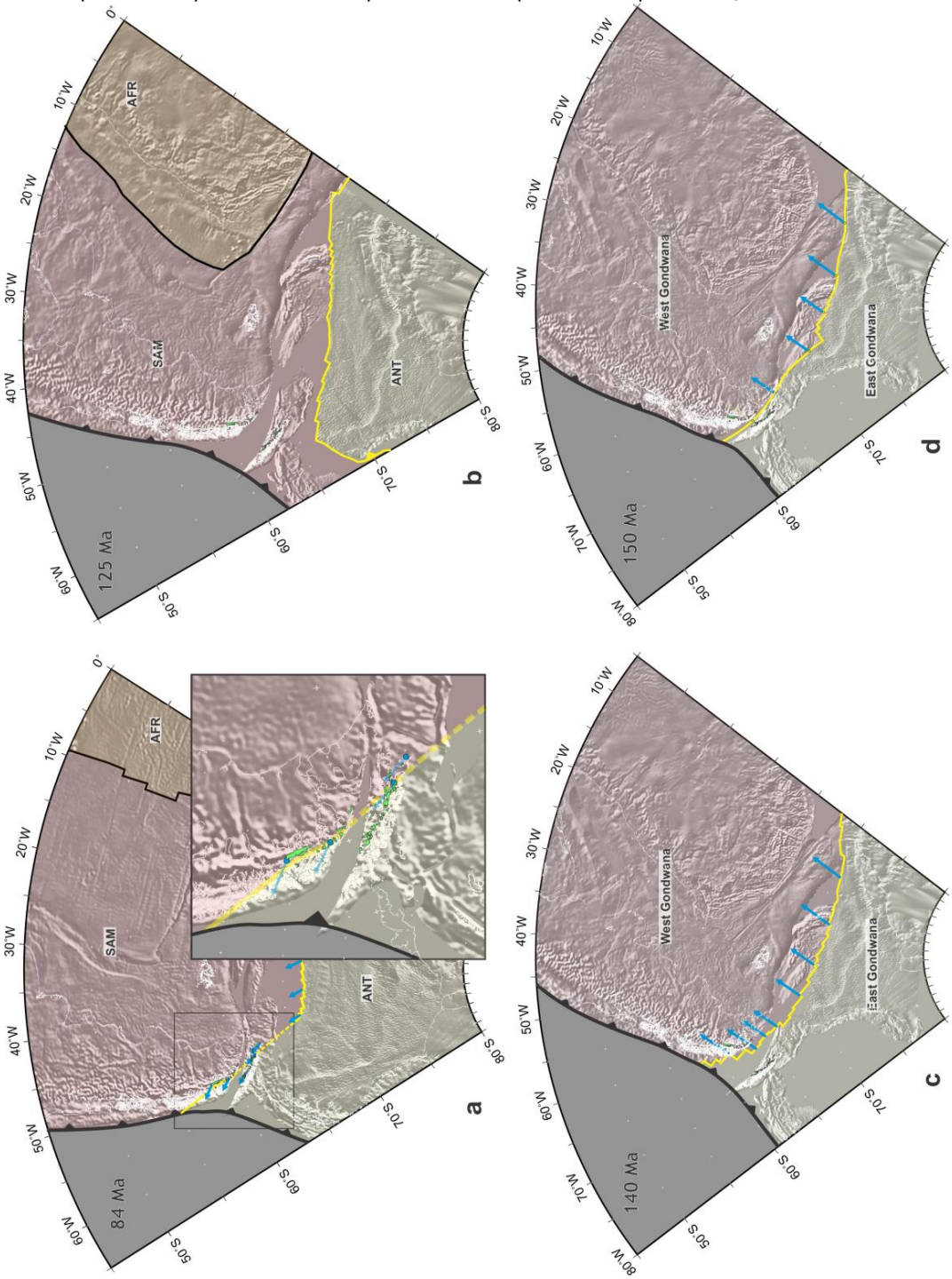

Figure 9. Closure of the SE part of the Rocas Verdes Basin (location in Figure 2). Red arrows: azimuth of motion of points on the South American (northern and eastern) side of the basin with respect to the Antarctic side in the period 94-84 Ma, calculated from Table 1. Violet arrow: azimuth in Paleocene times. Lines with barbs: thrust faults (after *Kraemer*, 2003). BF: Beagle Channel fault zone; MF: Magallanes-Fagnano fault zone. Dashed line: northern extent of the internal zone of the Fuegian fold and thrust belt. Green: basaltic and related rocks of the basin floor.

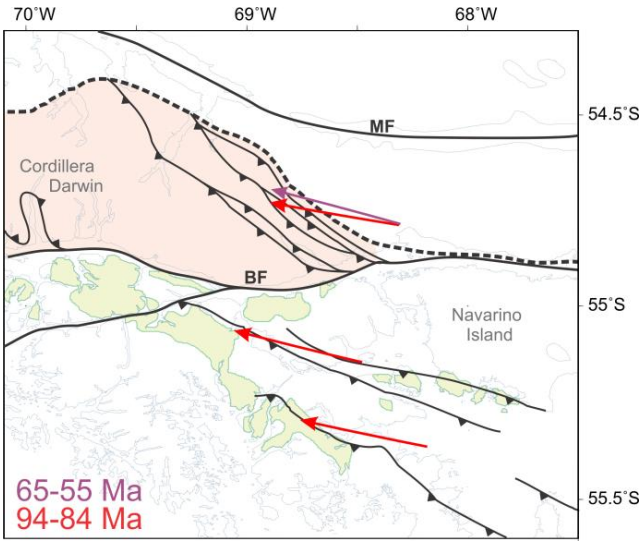

TABLES

Table 1. Solution finite rotations for Antarctica with respect to South America, from inversion of magnetic and flowline data in the Weddell Sea. Magnetic chrons from the *Cande and Kent* (1995) timescale. Rotations are right handed. Axes are those of the 95% confidence ellipsoid, and its orientation in degrees anticlockwise from east. Only the 95% confidence ellipses (axes 1 and 2 and azimuth) are depicted in figure 6.

Chron	Age (Ma)	Latitude	Longitude	Angle	95% ellipsoid			
					Axis 1	Axis 2	Axis 3	Azimuth
					1σ, great circle degrees			
3Ao	6.57	-78.75	152.15	1.25	2.30	0.16	0.032	80.51
5o	10.95	-79.00	166.63	2.82	6.92	2.09	0.030	89.42
5Co	16.73	-82.74	170.78	5.13	4.38	1.66	0.044	92.25
6o	20.13	-76.73	171.58	5.56	4.57	1.56	0.037	95.02
8o	26.55	-68.37	174.70	6.61	3.37	0.96	0.040	100.49
13y	33.06	-73.10	-176.64	9.80	3.06	0.57	0.062	108.76
18y	38.43	-72.32	-177.36	11.70	2.46	0.45	0.059	111.86
21P	47.07	-75.00	-161.60	15.01	1.70	0.32	0.087	122.25
25P	56.25	-77.77	-145.26	18.16	1.40	0.33	0.108	139.25
28P	63.63	-76.95	-139.32	19.13	1.35	0.29	0.138	139.74
30y	65.58	-77.47	-131.93	21.31	1.25	0.29	0.136	146.59
32y	71.07	-76.26	-133.12	22.62	1.20	0.23	0.127	144.22
33y	73.58	-75.67	-134.72	23.43	1.19	0.26	0.140	141.62
34y	83.5	-76.51	-123.73	28.54	1.01	0.19	0.126	151.03
I2	94[a]	-76.46	-113.91	33.01	1.29	0.27	0.143	166.69
MAU	107[a]	-75.92	-107.18	36.55	3.71	0.47	0.181	137.17
I	119[a]	-74.70	-100.72	39.86	0.95	0.18	0.113	170.10
34o	124.61	-72.33	-101.08	40.85	0.82	0.14	0.101	159.86
M5no	130.80	-70.64	-95.27	44.05	0.83	0.24	0.098	163.74
M11Ao	137.51	-66.62	-93.67	44.47	0.99	0.26	0.093	152.05
M14o	139.77	-63.89	-91.74	45.45	1.25	0.35	0.101	134.52
ORI	155-172[b]	-59.63	-89.51	46.17	2.34	0.36	0.115	133.68
FIT	172-183[b]	-52.38	-85.93	48.80	4.05	0.40	0.115	128.45

[a] Ages assigned based on assumption of zero change in spreading rate through the Cretaceous Normal Polarity Superchron

[b] See text